Astronomy
&
Astrophysics

The afterglow and the host galaxy of GRB 011211[*],[**],[***]

P. Jakobsson[1,2], J. Hjorth[1], J. P. U. Fynbo[1,3], J. Gorosabel[4,5], K. Pedersen[1], I. Burud[5], A. Levan[2,5], C. Kouveliotou[6], N. Tanvir[7], A. Fruchter[5], J. Rhoads[5], T. Grav[8], M. W. Hansen[8], R. Michelsen[1], M. I. Andersen[9], B. L. Jensen[1], H. Pedersen[1], B. Thomsen[3], M. Weidinger[3], S. G. Bhargavi[10], R. Cowsik[10], and S. B. Pandey[11]

[1] Astronomical Observatory, University of Copenhagen, Juliane Maries Vej 30, 2100 Copenhagen Ø, Denmark
[2] Department of Physics and Astronomy, University of Leicester, University Road, Leicester, LE1 7RH, UK
[3] Department of Physics and Astronomy, University of Aarhus, Ny Munkegade, 8000 Århus C, Denmark
[4] IAA-CSIC, PO Box 03004, 18080 Granada, Spain
[5] Space Telescope Science Institute, 3700 San Martin Drive, Baltimore, MD 21218, USA
[6] NSSTC, SD-50, 320 Sparkman Drive, Huntsville, Alabama 35805, USA
[7] Department of Physical Sciences, University of Hertfordshire, College Lane, Hatfield, Herts AL10 9AB, UK
[8] Institute of Theoretical Astrophysics, University of Oslo, PB 1029 Blindern, 05315 Oslo, Norway
[9] Astrophysikalisches Institut Potsdam, An der Sternwarte 16, 14482 Potsdam, Germany
[10] Indian Institute of Astrophysics, Sarjapur Road, Bangalore 560 034, India
[11] State Observatory, Manora Peak, Nainital 263 129, India

Abstract. We present optical, near-infrared, and X-ray observations of the optical afterglow (OA) of the X-ray rich, long-duration gamma-ray burst GRB 011211. Hubble Space Telescope (HST) data obtained 14, 26, 32, and 59 days after the burst, show the host galaxy to have a morphology that is fairly typical of blue galaxies at high redshift. We measure its magnitude to be $R = 24.95 \pm 0.11$. We detect a break in the OA R-band light curve which is naturally accounted for by a collimated outflow geometry. By fitting a broken power-law to the data we find a best fit with a break 1.56 ± 0.02 days after the burst, a pre-break slope of $\alpha_1 = -0.95 \pm 0.02$, and a post-break slope of $\alpha_2 = -2.11 \pm 0.07$. The UV-optical spectral energy distribution (SED) around 14 hours after the burst is best fit with a power-law with index $\beta = -0.56 \pm 0.19$ reddened by an SMC-like extinction law with a modest $A_V = 0.08 \pm 0.08$ mag. By comparison, from the XMM-Newton X-ray data at around the same time, we find a decay index of $\alpha_X = -1.62 \pm 0.36$ and a spectral index of $\beta_X = -1.21^{+0.10}_{-0.15}$. Interpolating between the UV-optical and X-ray implies that the cooling frequency is located close to $\sim 10^{16}$ Hz in the observer frame at the time of the observations. We argue, using the various temporal and spectral indices above, that the most likely afterglow model is that of a jet expanding into an external environment that has a constant mean density rather than a wind-fed density structure. We estimate the electron energy index for this burst to be $p \sim 2.3$.

Key words. cosmology: observations – gamma rays: bursts – stars: supernovae: general – ISM: dust, extinction

1. Introduction

A deceleration of a relativistic fireball in the surrounding environment is now widely believed to cause the afterglow emission of GRBs (see Piran 1999 for a review). The external

medium could be either a precursor wind from the GRB progenitor (Chevalier & Li 2000) or the interstellar medium (ISM) of the host galaxy (Waxman 1997). The interaction between the fireball and this ambient medium produces a shock that accelerates electrons and gives them a power-law distribution of ultra-relativistic energies, $N(\gamma) \propto \gamma^{-p}$, where p is the electron energy index. This leads to the production of synchrotron emission where the flux of the afterglow can be described by a power-law decline in time and frequency, $F \propto t^\alpha \nu^\beta$ (Sari et al. 1998). The decay rate, α, depends on the nature of the fireball and also on the density structure of the ambient medium. Light curves from observed afterglows typically have an initial decay index of $\alpha_1 \sim -1$, which often steepens 1–3 days after the GRB to $\alpha_2 \sim -2$ or even steeper (e.g. Fig. 4 in Andersen et al. 2000).

The GRB 011211 R-band light curve, presented by Holland et al. (2002, hereafter H02), showed the OA decaying as a power-law with a slope of $\alpha = -0.83 \pm 0.04$ for the first ~2 days after the burst at which time there was evidence for a break. Reeves et al. (2002, hereafter R02) found that the X-rays emitted in the wake of GRB 011211 originated in an extremely hot gas outflowing from the GRB progenitor at ~$0.1c$, and that this gas was highly enriched with the by-products of a supernova explosion.

In this paper we present photometry of the OA of GRB 011211, taken between ~0.6 and ~30 days after the burst occurred. We explore the properties of the X-ray light curve, observed between ~0.5 and ~0.85 days from the onset of the burst. We model the afterglow data and conclude that the most likely model is a jet expanding into an external environment with a constant mean density. We also analyse HST/STIS images in order to derive the photometric properties of the host galaxy.

The organization of this paper is as follows. The optical and near-infrared (NIR) observations are presented in Sect. 2. In Sect. 3 we analyze HST/STIS images of the OA and the host galaxy. In Sects. 4 and 5 we investigate the optical and X-ray light curves. The spectral energy distribution (SED) of the afterglow along with the derived extinction is discussed in Sect. 6. We use the derived properties of the OA in Sect. 7 to compare our results with afterglow models. Finally, Sect. 8 summarises the main results. Throughout this paper, we adopt a Hubble constant of $H_0 = 65$ km s^{-1} Mpc^{-1} and assume $\Omega_m = 0.3$ and $\Omega_\Lambda = 0.7$.

2. Ground-based observations

GRB 011211 was detected by the Italian/Dutch satellite BeppoSAX on 2001 Dec. 11.7982 UT. A $5'$ radius error circle was circulated via the GRB Coordinate Network (GCN)[1] 5.4 h after the burst (Gandolfi 2001a). Less than 2 h later the error radius was refined to only $2'$ (Gandolfi 2001b). This X-ray rich GRB had a duration of approximately 270 s, making it one of the longest duration bursts observed by BeppoSAX and thus placing it firmly in the "long-duration" burst category.

The OA was discovered at the Nordic Optical Telescope (NOT) (Grav et al. 2001; Jakobsson et al. 2003, hereafter J03) on 2001 Dec. 12.2 UT, 9.6 h after the burst. A NOT image of the OA and its surrounding field is displayed in Fig. 1. The OA was monitored during the following week with the NOT and with the Danish 1.54-m telescope at La Silla (Jensen et al. 2001b). The decline of the OA was also observed at several other telescopes (Soszynski et al. 2001; Bhargavi & Cowsik 2001; Holland et al. 2001). In India the follow-up observations of the OA were carried out between 2001 Dec. 12–14, using the 2.34-m Vainu Bappu Telescope (VBT) as well as the 1-m Zeiss telescope of the Vainu Bappu Observatory (VBO), and on 2001 Dec. 12, using the 1-m Sampurnanda telescope at the State Observatory (SO). In addition, the 3.58-m New Technology Telescope (NTT) at La Silla was used to obtain NIR images of the OA shortly after the burst, while R-band images ~5.5
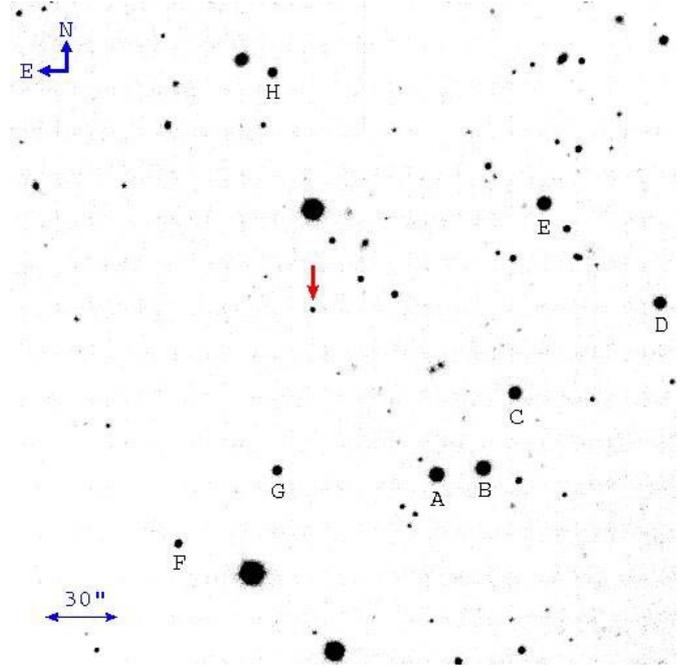
Fig. 1. An R-band image of the GRB 011211 optical afterglow. The position of the optical afterglow is marked with an arrow. Also marked are the eight secondary calibration stars A–H used to transform the relative photometry onto the standard system. The photometric properties of these stars are given in Table 2.

and ~9.5 days after the burst were obtained at the Melipal and Yepun of the 8.2-m Very Large Telescope (VLT) as part of the GRACE[2] program. The journal of our observations is listed in Table 1.

The redshift of the burst was measured to be $z = 2.140$ via absorption lines in an optical spectrum taken at the Yepun of the VLT (Fruchter et al. 2001). This redshift was confirmed with spectra obtained at the Magellan 6.5-m Walter Baade telescope (Gladders et al. 2001; H02) and with the 3.5-m Telescopio Nazionale Galileo (Fiore et al. 2001).

3. Observations from space

In an XMM-Newton follow-up observation (0.51–0.84 days after the GRB trigger) a source in the BeppoSAX error box was detected (Santos-Lleo et al. 2001). Subsequent analysis showed this source to be fading with a decay index $\alpha_X = -1.7 \pm 0.2$ in the 0.2–10 keV band (R02).

We have reduced the publicly available HST data[3] taken ~14 (epoch 1), ~26 (epoch 2), ~32 (epoch 3) and ~59 (epoch 4) days after the burst (Fig. 2). The dithered data were pre-processed using the "on the fly" calibration from the HST archive[4] and were drizzled onto a final output grid with pixels half the size of the original input pixels using a value for `pixfrac` of 0.7 (Fruchter & Hook 2002). In order to convert the 50CCD (clear, hereafter referred to as CL) broadband

---

[1] http://gcn.gsfc.nasa.gov/gcn/

[2] GRB Afterglow Collaboration at ESO.
[3] HST proposal 8867 (S. Kulkarni).
[4] http://archive.stsci.edu

Table 1. The journal of the GRB 011211 observations and the results of the photometry. Upper limits are 2σ in a circular aperture with radius $2''$. No corrections for extinction have been applied to the photometry in the table. The flux from the host galaxy has not been subtracted.

Date (UT) of 2001 Dec.[a]	Obs.	Magnitude	Seeing (arcsec)	Exp. time (s)
U-band:				
13.2467	NOT	21.5 ± 0.3	1.20	3×600
B-band:				
12.9819	VBT	21.914 ± 0.108	2.5	1800
13.2280	NOT	22.241 ± 0.076	1.55	3×300
13.3382	1.54-m	22.287 ± 0.068	1.00	3×600
13.9550	VBT	23.06 ± 0.27	3.00	2×1200
V-band:				
12.9403	VBT	21.522 ± 0.077	3.00	1200
12.9569	VBT	21.575 ± 0.073	2.44	1200
13.2189	NOT	21.478 ± 0.111	1.55	300
13.3044	1.54-m	21.757 ± 0.089	1.00	3×300
13.9180	VBT	22.82 ± 0.22	2.80	2×900
20.3087	1.54-m	25.00 ± 0.22	1.35	7×1200
R-band:				
12.8722	VBT	20.91 ± 0.13	2.20	600
12.8872	VBT	21.022 ± 0.089	2.20	900
12.9007	VBT	20.732 ± 0.081	2.10	600
12.9097	VBT	20.952 ± 0.092	2.10	600
12.9188	VBT	20.959 ± 0.094	2.10	600
12.9271	VBT	21.061 ± 0.129	2.10	600
12.9399	VBO	21.204 ± 0.168	2.70	900
12.9602	SO	21.037 ± 0.067	3.40	3×300
12.9753	VBO	21.203 ± 0.163	2.10	900
12.9785	SO	21.174 ± 0.047	3.40	2×600
12.9945	SO	21.134 ± 0.063	3.40	2×600
12.9979	VBT	21.100 ± 0.110	2.30	600
13.0108	SO	21.195 ± 0.088	3.40	2×600
13.2096	NOT	21.123 ± 0.076	1.10	300
13.2843	1.54-m	21.378 ± 0.067	1.20	600
13.2924	1.54-m	21.408 ± 0.062	0.95	600
13.3550	1.54-m	21.356 ± 0.057	0.85	600
13.3631	1.54-m	21.495 ± 0.086	0.95	600
15.3438	1.54-m	>23.0	1.15	$1200 + 900$
16.3071	1.54-m	23.32 ± 0.25	1.30	7×1200
17.3031	1.54-m	23.69 ± 0.25	1.80	6×1200
17.3075	VLT	24.1 ± 0.2	1.30	1800
18.3044	1.54-m	24.22 ± 0.40	1.10	6×1200
21.3080	VLT	25.27 ± 0.16[b]	0.70	3600
25.8190	HST	26.71 ± 0.16[b]	—	5193
6.7720	HST	27.45 ± 0.21[b]	—	4785
12.712	HST	28.40 ± 0.48[b]	—	4785
I-band:				
12.9879	VBO	20.92 ± 0.21	2.60	900
13.2143	NOT	20.99 ± 0.23	1.00	300
13.3237	1.54-m	20.86 ± 0.15	0.90	3×300
15.3069	1.54-m	22.75 ± 0.25	1.15	4×900
20.2350	1.54-m	>23.2	1.25	$3 \times 900 + 500$
J-band:				
12.3616	NTT	19.34 ± 0.05	1.05	900
14.3470	NTT	21.04 ± 0.05	0.55	2700
K-band:				
12.3736	NTT	18.02 ± 0.07	0.90	840

[a] For the last two HST data points the date is 2002 January.
[b] OA magnitude.
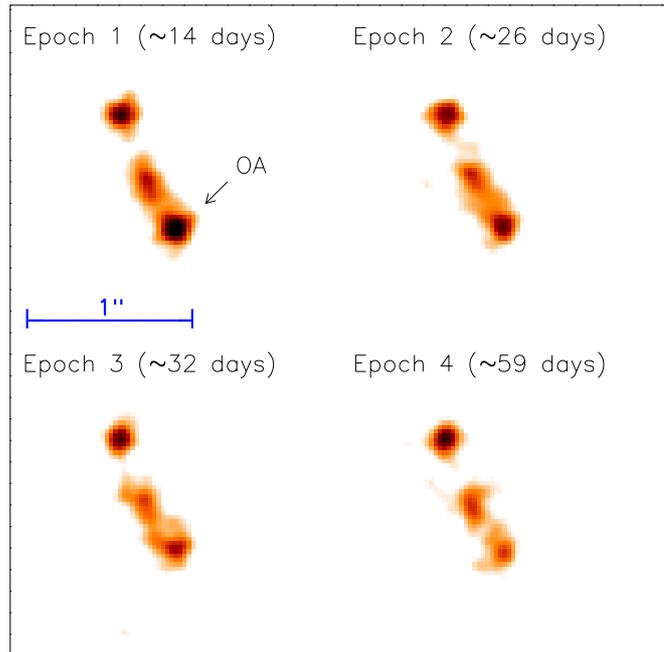
Fig. 2. HST images centered on the host galaxy at four different epochs showing the decline of the optical afterglow. North is up and east is to the left. The numbers in the parentheses indicate the time after the burst.

STIS magnitude to an R-band magnitude we assumed a power-law spectrum of $\beta = -0.56 \pm 0.19$ as derived in Sect. 6. We note that the magnitude errors quoted include a term due to this colour correction since the late time colour is poorly constrained. This colour term would not normally be expected to change substantially for a GRB afterglow, however an underlying supernova can lead to significant reddening of the normally blue afterglow spectrum. In practice this effect will be of the order of 0.1 mags in changing the power-law from that observed to $\sim\nu^{-3}$, and hence our corrections to an R-band magnitude allow for this possibility. In order to calculate the magnitude of the OA we subtracted the epoch 4 image from the previous three images and then performed aperture photometry. To avoid any contamination from the OA in the final HST image, we subtracted from it the expected OA magnitude (see Sect. 4.2 and the dotted line in Fig. 3). The host galaxy seems to have a multi-component morphology, similar to the host of GRB 000926 (Fynbo et al. 2002) and many other high-z galaxies (e.g. Giavalisco et al. 1996; Møller et al. 2002). Recent Lyα observations (Fynbo et al. 2003) have revealed that all the components are related to the host, with most of the Lyα emission emitted from the source north of the OA position.

Using a large ($1''$) aperture we estimated the total magnitude of the host galaxy complex in our broadband STIS image to be $CL \sim 25.60 \pm 0.05$. In order to calculate the R-magnitude of the host we estimated a colour correction based on the colours of other GRB host galaxies (e.g. Sokolov et al. 2001). Allowing for Galactic reddening in the direction of GRB 011211, $E(B-V) = 0.045$ from Schlegel et al. (1998), the range of reasonable colour corrections ($R - V$) for this host lies between -0.75 and -0.55. We adopted the centre of this range

Table 2. *BVRI* magnitudes (Henden 2001b) for the eight secondary calibration stars A–H (see Fig. 1).

Star	B	V	R	I
A	17.292 ± 0.011	16.392 ± 0.011	15.838 ± 0.014	15.310 ± 0.020
B	17.507 ± 0.008	16.481 ± 0.008	15.849 ± 0.015	15.303 ± 0.048
C	19.069 ± 0.034	17.520 ± 0.034	16.441 ± 0.038	15.056 ± 0.060
D	17.824 ± 0.015	17.158 ± 0.008	16.744 ± 0.015	16.401 ± 0.019
E	17.128 ± 0.009	16.479 ± 0.008	16.096 ± 0.020	15.706 ± 0.043
F	20.874 ± 0.129	19.446 ± 0.036	18.389 ± 0.055	17.186 ± 0.061
G	18.479 ± 0.016	18.002 ± 0.011	17.705 ± 0.021	17.383 ± 0.104
H	18.768 ± 0.060	18.130 ± 0.040	17.783 ± 0.046	17.304 ± 0.183

(−0.65 mag) as the correction for the host of GRB 011211. This implies that the *R*-magnitude of the host is 24.95 ± 0.11. We note that this is a somewhat crude estimate since the exact colour profile of the host is unknown. The results of the OA photometry are presented in Table 1.

4. The optical light curve

### 4.1. Construction of the R-band light curve

We measured the magnitude of the OA relative to 8 stars in the field. The calibrated magnitudes of these stars are given in Henden (2001a,b) and shown in Table 2. In some of our images we only used a subset of these 8 stars due to saturation. We used aperture photometry in a circular aperture with radius 2″ in order to fully include the emission from the host galaxy reported by Burud et al. (2001). Finally, we used our HST results to subtract the host contribution from each data point.

4.2. Power-law fitting

Our *R*-band light curve is shown in Fig. 3. It is supplemented by early light curve data points from H02 and J03. Also plotted is a broken power-law fit to the light curve prior to day 10. From the formal best fit we find that the initial light curve decay has a power-law index of $\alpha_1 = -0.95 \pm 0.02$, while $\alpha_2 = -2.11 \pm 0.07$, with the break occurring at $t_b = 1.56 \pm 0.02$ days ($\chi^2_{43} = 7.82$, where $\chi^2_{\text{d.o.f.}} = \chi^2/\text{degree of freedom}$, is the reduced χ^2 of the fit). Neither the three HST points, nor the two upper limits were included in this fit. In the case of the HST points, there is a risk of contamination from a possible supernova (SN) bump, however, including them does not affect α_1 or t_b, and α_2 only changes to -2.13 ± 0.04.

The broken power-law fits are formally strongly rejected by the data due to the wiggles in the early light curve (see H02 and J03). These short-term variations make the fitted value of α_1 dependent on the sampling of the light curve. This is reflected in the formally inconsistent value $\alpha_1 = -0.83 \pm 0.04$ obtained by H02, who had a very different sampling of the early light curve. The true uncertainty in α_1 is therefore more likely around 0.10. The rapid variations present in the early light curve are explored in J03.

We note that there is an indication of a bump in the light curve around 26 days after the burst, corresponding to ~8 days
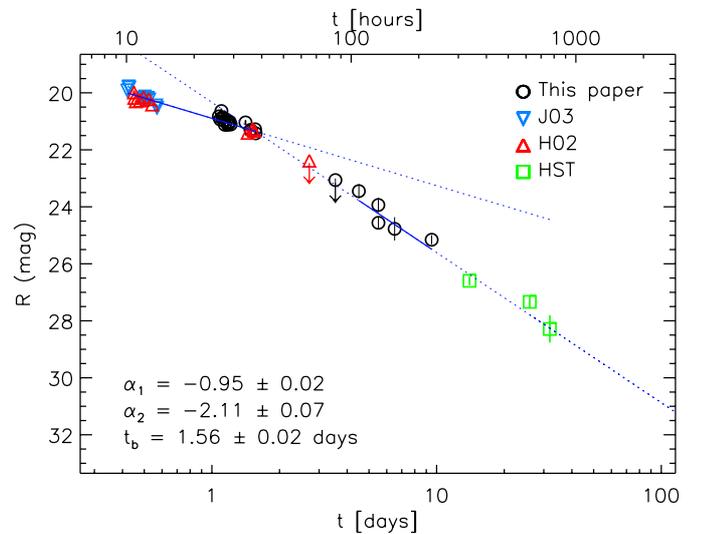
Fig. 3. The *R*-band light curve of the OA based on the measurements given in Table 1 (circles), the data presented in H02 (triangles) and J03 (upside down triangles), and publicly available HST data (squares). All data points have been corrected for Galactic reddening. The dotted lines are extrapolation of the straight lines fit through the light curves.

in the restframe. This corresponds to an extra contribution to the flux of the expected smooth power-law decay of $CL = 28.92 \pm 0.45$. It is unclear whether a SN could produce such a bump since Kirshner et al. (1993) find very little flux below a restframe wavelength of ~2900 Å for a well studied type Ia SN.

5. The X-ray light curve

The observations of GRB 011211 by the orbiting XMM-Newton X-ray telescope started on 2001 Dec. 12.30, ~12 h after the GRB. We have analyzed data from the European Photon Imaging Camera (EPIC), using both the MOS and pn instruments. The total observation had a duration of 29.8 ks for the EPIC-pn detector, providing most of the X-ray photons from the afterglow.

The data were extracted from the Science Operations homepage[5]. In order to produce a clean light curve the data were screened according to the following criteria: (i) only good

---

[5] `http://xmm.vilspa.esa.es/external/xmm_news/items/grb011211/index.shtml`

X-ray events with single and double pixel events were included, (ii) only events in the well calibrated energy range 0.5–10 keV were included, and (iii) finally a few short periods (much shorter than the time scale of the variations seen in the light curve) affected by high background were excluded. Applying these criteria a light curve was extracted for each detector from a circular region with a radius of 40″ centered on the X-ray afterglow. Background light curves for each detector were produced from two circular regions with a radius of 40″ and centered at the same distance from the nearest chip gap as the X-ray afterglow. For each of the three detectors the two background light curves were identical within the uncertainties. The EPIC-pn afterglow flux was corrected for flux falling on a chip gap in the initial 1.22 h of the observation and during the subsequent 770 s repointing. Likewise, the background subtracted light curves from the three detectors showed consistent features and a merged, background subtracted light curve was produced.

A power-law was fit through the X-ray light curve. The overall flux decays during the observation with a decay index of $\alpha_X = -1.96 \pm 0.16$, consistent with the value found by R02. As detailed in J03, the first two hours in the X-ray light curve are most likely affected either by energy variations within the expanding jet, or by emission line features (R02). The X-ray decay slope increases to $\alpha_X = -1.62 \pm 0.36$ if the initial two hours are omitted from the fit.

In order to compare the optical SED (see Sect. 6) to the X-ray spectrum, we extracted a 10 ks spectrum from the EPIC-pn detector centered at Dec. 12.37. EPIC-pn data were extracted as described above, and a power-law with absorption fixed at the Galactic value was fit to the spectrum. This model is a good fit to the spectrum and absorption in excess of the Galactic value is not required. The best fit spectral index is $\beta_X = -1.21^{+0.10}_{-0.15}$, and the X-ray spectrum above 1 keV (which is unaffected by absorption) is shown in the inset of Fig. 4.

6. Spectral energy distribution of the afterglow

In order to estimate the SED of the afterglow and the value of the spectral slope we used the *UJK* data in Table 1 along with *BVRI* data from J03. We interpolated the magnitudes to a common epoch, Dec. 12.3681 (0.5699 days after the burst), taking into account the short-term variations present in the optical light curve (see J03). We note that the flux from the host galaxy (estimated in Sect. 3) has not been subtracted. However, the host is faint enough that it will contribute only ≈2% of the flux at the epoch we are exploring. Therefore, we believe that the flux from the host galaxy does not significantly affect our results. The SED was constructed as explained in Fynbo et al. (2001). The result is shown in Fig. 4, where we have corrected the data for Galactic reddening using the reddening maps of Schlegel et al. (1998). The fact that the SED is similar to those of other afterglows at similar redshifts (Jensen et al. 2001a; Fynbo et al. 2001; Holland et al. 2003) strengthens the validity of our interpolation approach.

In order to quantify the effects of extinction, we have in Fig. 4 fit the function $F_\nu \propto \nu^{-\beta} \times 10^{-0.4 A_\nu}$ to the SED, where A_ν is the extinction in magnitudes at frequency ν. We have
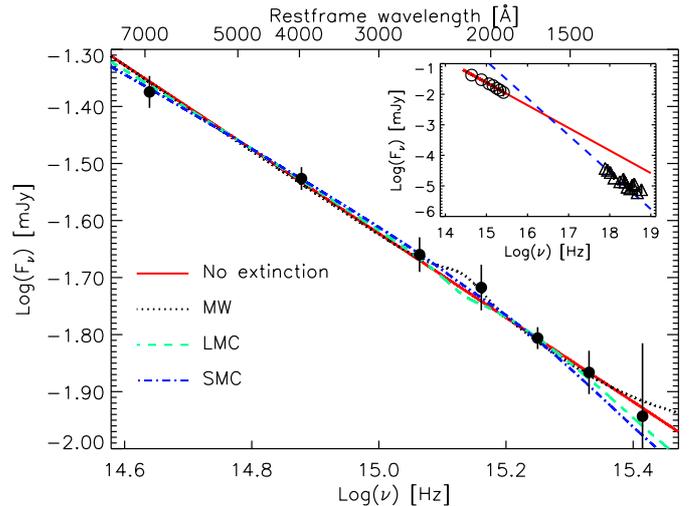
Fig. 4. The spectral energy distribution (SED) of the GRB 011211 afterglow. The data points are based on the *UBVRIJK*-band observations carried out at the NOT, Danish 1.54-m and the NTT around Dec. 12.3681 (see Table 1 and J03). The abscissa displays the frequency/wavelength in the GRB restframe. The SED is well fit by an underlying $\beta = -0.56$ power-law with an SMC extinction law with $A_V = 0.08$. The inset shows the *UBVRIJK*-band observations (open rings) along with the X-ray spectrum (open triangles) on Dec. 12.37. The solid line is a pure power-law fit to the optical while the dashed line is a pure power-law fit to the X-ray data points.

Table 3. Fits to the GRB 011211 afterglow SED. We note that $\chi^2_{d.o.f.} = \chi^2/$degree of freedom, is the reduced χ^2 of the fit. The low value of $\chi^2_{d.o.f.}$ in all fits may indicate that we have overestimated the errors.

Fitting function	$\chi^2_{d.o.f.}$	β	A_V
No extinction	0.38	-0.74 ± 0.05	0
MW	0.38	-0.82 ± 0.15	-0.07 ± 0.12
LMC	0.40	-0.60 ± 0.28	0.08 ± 0.16
SMC	0.25	-0.56 ± 0.19	0.08 ± 0.08

considered the three extinction laws (A_ν as a function of ν) given by Pei (1992), i.e. for the Milky Way (MW), Large Magellanic Cloud (LMC), and Small Magellanic Cloud (SMC). The latter two are particularly interesting since they have lower abundances of heavy elements and dust than the MW. In this respect, they may resemble galaxies at high redshifts, which are presumably in early stages of the chemical enrichment. In these three cases the dependence of the extinction with ν has been parameterized in terms of (restframe) A_V. Thus, the fits allow us to determine β and A_V simultaneously. Finally, we also considered the no-extinction case where $F_\nu \propto \nu^{-\beta}$.

The parameters of the fits are shown in Table 3. For the no-extinction case we find a value of β consistent with the one found by H02 ($\beta = -0.61 \pm 0.15$). On the other hand, the best fit was achieved for the SMC extinction law, where we derive a modest extinction of $A_V = 0.08 \pm 0.08$ (restframe *V*) and a spectral index of $\beta = -0.56 \pm 0.19$.

For the redshift of the GRB 011211 the interstellar extinction bump at 2175 Å is shifted close to the *R*-band.

Table 4. Calculation of the closure relation, $|\alpha_1| + b|\beta| + c$, for two afterglow models. The closure relation will have a value of zero for a successful model. The ISM and wind models are for isotropic expansion in a homogeneous and wind-stratified medium, respectively. The electron energy power-law index, p, is written as a function of the observed β, while $\Delta\alpha$ is calculated from p.

Model	ν_c	(b, c)	Closure	p	$\Delta\alpha$
ISM	$\nu_c > \nu_o$	$(-3/2, 0)$	0.11 ± 0.29	$1 - 2\beta = 2.12 \pm 0.38$	$(p + 3)/4 = 1.28 \pm 0.10$
ISM	$\nu_c < \nu_o$	$(-3/2, 1/2)$	0.61 ± 0.29	$-2\beta = 1.12 \pm 0.38$	$(p + 2)/4 = 0.78 \pm 0.10$
Wind	$\nu_c > \nu_o$	$(-3/2, -1/2)$	-0.39 ± 0.29	$1 - 2\beta = 2.12 \pm 0.38$	$(p + 1)/4 = 0.78 \pm 0.10$
Wind	$\nu_c < \nu_o$	$(-3/2, 1/2)$	0.61 ± 0.29	$-2\beta = 1.12 \pm 0.38$	$(p + 2)/4 = 0.78 \pm 0.10$

This extinction feature is very prominent for the MW, moderate in the LMC, and almost nonexistent for the SMC extinction curve. Our data sampling makes it difficult to infer about the presence of a redshifted 2175 Å absorption bump in the *R*-band. However, the best MW fit implies an unphysical negative extinction (see Table 3). This result is further strengthened by the fact that the SMC is consistently a much better fit than the MW for GRBs where these fits have been applied (GRB 000301C: Jensen et al. 2001a; Rhoads & Fruchter 2001; GRB 000926: Fynbo et al. 2001; GRB 021004: Holland et al. 2003).

Our best-fit extinction model is consistent with a zero extinction. This result is strengthened by the fact that the X-ray spectrum implies no significant absorption in the host galaxy (Pedersen et al. 2003). Furthermore, the A_V value estimated from the *UBVRIJK*-band SED is (although close to the actual value) an upper limit of A_V. This is because the unextincted optical/NIR SED segment is not an idealized pure power-law (Sari et al. 1998), as there could be some shallow intrinsic curvature due to the proximity of ν_c to the *U*-band (Granot & Sari 2002). In conclusion, the data support a scenario of a host with a low intrinsic extinction and which is in the early stages of chemical enrichment.

7. Comparison with afterglow models

The parameters α_1, α_2 and t_b, and β can be used to investigate the physical mechanisms responsible for the break and the nature of the ambient medium in which the burst occurred. Breaks have been observed in many GRB light curves to date. They have been interpreted as evidence that the outflows from the bursts are collimated with opening angles of approximately $5°$–$10°$ (e.g. Rhoads 1999; Sari et al. 1999; Castro-Tirado et al. 1999; Holland et al. 2000). If GRBs are collimated outflows, the total energy requirement drops by a factor of between roughly 100 and 1000, providing a solution to the so-called "energy crisis" of GRBs.

The decay and spectral slopes depend on the electron energy distribution index p. This led Price et al. (2002) and Berger et al. (2002) to introduce the so-called closure relation, in order to distinguish between various afterglow models. Its exact representation depends on the definition of α_1, α_2 and β. In our notation $|\alpha_1| + b|\beta| + c = 0$, where the values of b and c depend on the location of the cooling frequency, ν_c, relative to the optical/NIR bands, ν_o, at the epoch of the observations. We use the spectral index found in Sect. 6, $\beta = -0.56 \pm 0.19$, which has been corrected for host extinction. Table 4 lists two models

used in the closure relation in order to explore the GRB environment before the observed break in the light curve: (i) expansion into a homogeneous medium, and (ii) expansion into a wind-fed medium.

Models with $\nu_c < \nu_o$ are disfavoured by the data. This result is further strengthened by the fact that α_X (the X-ray decay index, see Sect. 5) is steeper than α_1. This implies that there is a spectral break between the optical and X-rays. In addition, our observations imply that the difference between the low- and high-energy slopes is $\beta - \beta_X = 0.65^{+0.21}_{-0.24}$, consistent with the prediction of 0.5 in the standard synchrotron model (in the slow cooling regime). This result is displayed in the inset of Fig. 4. At the time of the measurements the cooling frequency is observed to be positioned close to $\sim 10^{16}$ Hz in the observer frame.

Only the ISM ($\nu_c > \nu_o$) model produces a closure consistent with zero. In Table 4 we also estimate $\Delta\alpha = \alpha_1 - \alpha_2$ for the afterglow models. The observed value of $\Delta\alpha = 1.16 \pm 0.07$ clearly favours the ISM ($\nu_c > \nu_o$) model. We note that each spectral or temporal power-law index relates to a certain value of p, and the correct model should result in a similar p for all indices. In our favoured model we get $p(\alpha_1) = 2.27 \pm 0.03$, $p(\alpha_2) = 2.11 \pm 0.07$, $p(\beta) = 2.12 \pm 0.38$, $p(\beta_X) = 2.4^{+0.2}_{-0.3}$, and $p(\alpha_X) = 2.8 \pm 0.5$. For the X-ray temporal slope we have used $\alpha_X = -1.62 \pm 0.36$ in order to avoid the influence of the short-term variations (see Sect. 5).

We note that $\alpha_X = -1.62 \pm 0.36$ is inconsistent with α_2, which makes a chromatic break due to the cooling frequency moving through the optical band (Covino et al. 2002) inconsistent with the data. Hence, the break in the optical light curve is indeed most likely due to a collimated outflow geometry.

The opening angle, θ_0, at the time of the break can be estimated using Eq. (2) in Frail et al. (2001). Using the same assumptions as H02 ($\eta_\gamma = 0.2$ and $n = 0.1$ cm^{-3}) leads to $\theta_0 = 3.4° \pm 0.1°$ for $t_b = 1.56 \pm 0.02$ days. From this we estimate that the total beamed energy in gamma-rays for GRB 011211 was $E_\gamma \approx 1.2 \times 10^{50}$ erg, after correcting for the beam geometry. This energy is in the low end of the distribution of the "standard" total beamed energy in gamma-rays centred on 1.3×10^{51} erg (Bloom et al. 2003). As pointed out by Bloom et al. (2003), modeling yields estimates in the range 0.1 cm$^{-3} \lesssim n \lesssim 30$ cm^{-3}, with little support for extremes of either high or low density. Assuming $n = 30$ cm^{-3} still gives a relatively low energy, $E_\gamma \approx 5 \times 10^{50}$ erg (with $\theta_0 \approx 6.9°$), compared to the median energy of 1.3×10^{51} erg.

8. Discussion

We have detected a break in the optical light curve of GRB 011211. Our observations imply $(\alpha_1, \alpha_2) = (-0.95 \pm 0.02, -2.11 \pm 0.07)$, with a break time of $t_b = 1.56 \pm 0.02$ days. The SED at December 12.37 reveals an SMC-like extinction in the host galaxy at the modest level of $A_V = 0.08 \pm 0.08$, with $\beta = -0.56 \pm 0.19$. These properties of the light curve could be explained by a jet expanding into an ambient medium that has a constant mean density. We estimate that $\theta_0 \approx 3.4°$–$6.9°$ at the time of the break, which reduces the energy released by the GRB by a factor of ~100–600 to $(1.2–5) \times 10^{50}$ erg.

Using HST/STIS data we estimate the host magnitude to be $R = 24.95 \pm 0.11$, a representative value for host galaxies which typically measure $R = 24$–26 (see e.g. Bloom et al. 2002).

Finally, we use the various relationships between the light curve decay indices (α_1, α_2 and α_X) and the spectral indices (β and β_X) with the electron energy index (p) to calculate five independent values of the latter. We get an average value of ~2.3, consistent with other bursts that seem to be adequately fit with models where $p \approx 2.3$–2.5 (van Paradijs et al. 2000).

References

Andersen, M. I., Hjorth, J., Pedersen, H., et al. 2000, A&A, 364, L54
Berger, E., Kulkarni, S. R., Bloom, J. S., et al. 2002, ApJ, 581, 981
Bhargavi, S., & Cowsik, R. 2001, GCN#1202
Bloom, J. S., Kulkarni, S. R., & Djorgovski, S. G. 2002, AJ, 123, 1111
Bloom, J. S., Frail, D. A., & Kulkarni, S. R. 2003, ApJ, in press [astro-ph/0302210]
Burud, I., Rhoads, J., Fruchter, A., & Hjorth, J. 2001, GCN#1213
Castro-Tirado, A. J., Zaptero-Osorio, M. R., & Caon, N., et al. 1999, Science, 283, 2069
Chevalier, R. A., & Li, Z. Y. 2000, ApJ, 536, 195
Covino, S., Lazzati, D., Malesani, D., et al. 2002, A&A, 392, 865
Fiore, F., Israel, G. L., Antonelli, L. A., et al. 2001, GCN#1203
Frail, D. A., Kulkarni, S. R., Sari, R., et al. 2001, ApJ, 562, L55
Fruchter, A., Vreeswijk, P., Rhoads, J., & Burud, I. 2001, GCN#1200
Fruchter, A. S., & Hook, R. N. 2002, PASP, 114, 144
Fynbo, J. P. U., Gorosabel, J., Dall, T. H., et al. 2001, A&A, 373, 796
Fynbo, J. P. U., Møller, P., Thomsen, B., et al. 2002, A&A, 388, 425
Fynbo, J. P. U., Jakobsson, P., Møller, P., et al. 2003, A&A, 406, L63
Gandolfi, G. 2001a, GCN#1188
Gandolfi, G. 2001b, GCN#1189
Giavalisco, M., Steidel, C. C., & Macchetto, F. D. 1996, AJ, 470, 189
Gladders, M., Holland, S., Garnavich, P. M., et al. 2001, GCN#1209
Granot, J., & Sari, R. 2002, ApJ, 568, 820
Grav, T., Hansen, M. W., Pedersen, H., et al. 2001, GCN#1191
Henden, A. 2001a, GCN#1197
Henden, A. 2001b, GCN#1303
Holland, S., Björnsson, G., Hjorth, J., & Thomsen, B. 2000, A&A, 364, 467
Holland, S., Berlind, P., Bersier, D., et al. 2001, GCN#1204
Holland, S., Soszyński, I., Gladders, M., et al. 2002, AJ, 124, 639 (H02)
Holland, S., Weidinger, M., Fynbo, J. P. U., et al. 2003, AJ, 125, 2291
Jakobsson, P., Hjorth, J., Ramirez-Ruiz, E., et al. 2003, ApJ, submitted (J03)
Jensen, B. L., Fynbo, J. P. U., Gorosabel, J., et al. 2001a, A&A, 370, 909
Jensen, B., Pedersen, H., Hjorth, J., et al. 2001b, GCN#1195
Kirshner, R. P., Jeffery, D. J., Leibundgut, B., et al. 1993, ApJ, 415, 589
Møller, P., Warren, S. J., Fall., S. M., Fynbo, J. P. U., & Jakobsen, P. 2002, ApJ, 574, 51
Pedersen, K., et al. 2003, ApJ, in preperation
Pei, Y. C. 1992, ApJ, 395, 130
Piran, T. 1999, Phys. Rep., 314, 575
Price, P. A., Berger, E., Reichart, D. E., et al. 2002, ApJ, 572, L51
Reeves, J. N., Watson, D., Osborne, J. P., et al. 2002, Nature, 416, 512 (R02)
Rhoads, J. E. 1999, ApJ, 525, 737
Rhoads, J. E., & Fruchter, A. 2001, ApJ, 546, 117
Santos-Lleo, M., Loiseau, N., Rodriguez, P., Altieri, B., & Schartel, N. 2001, GCN#1192
Sari, R., Piran, T., & Narayan, R. 1998, ApJ, 497, L17
Sari, R., Piran, T., & Halpern, J. P. 1999, ApJ, 519, L17
Schlegel, D. J., Finkbeiner, D. P., & Davis, M. 1998, ApJ, 500, 525
Sokolov, V. V., Fatkhullin, T. A., Castro-Tirado, A. J., et al. 2001, A&A, 372, 438
Soszynski, I., Holland, S., Garnavich, P., et al. 2001, GCN#1199
van Paradijs, J., Kouveliotou, C., & Wijers, R. A. M. J. 2000, ARA&A, 38, 379
Waxman, E. 1997, ApJ, 485, L5